Repurposing disulfiram (Tetraethylthiuram Disulfide) as a potential drug candidate against *Borrelia burgdorferi in vitro and in vivo*

Short Title: Disulfiram effective drug against *Borrelia burgdorferi*

Hari-Hara SK Potula[1], Jahanbanoo Shahryari[1], Mohammed Inayathullah[1], Andrey Victorovich Malkovskiy[2], Kwang-Min Kim[1] and Jayakumar Rajadas[1]*

[1]Biomaterials and Advanced Drug Delivery, Stanford Cardiovascular Pharmacology Division, Cardiovascular Institute, Stanford University School of Medicine, Palo Alto, California, 94304, USA.

[2]Carnegie Institute for Science, Department of Plant Biology, Stanford University, Palo Alto, California, 94305, USA.

*Corresponding author: Jayakumar Rajadas: 1050 Arastradero Road, Building A, Room A148, Palo Alto, CA 94304. Phone: (650) 724-6806 Fax: (650) 724-4694.

Email: jayraja@stanford.edu.

25 **Keywords**: Lyme disease, *Borrelia burgdorferi*, antimicrobial activity, disulfiram, Lyme

26 carditis.

27 ABSTRACT

28 Lyme disease caused by the *Borrelia burgdorferi* (*Bb or B. burgdorferi*) is a most common

29 vector-borne, multi-systemic disease in USA. Although, most Lyme disease patients can be

30 cured with a course of antibiotic treatment, a significant percent of patient population fail to be

31 disease-free post-treatment, necessitating the development of more effective therapeutics. We

32 previously found several drugs including disulfiram having with good activity against *B.*

33 *burgdorferi*. In current study, we evaluated the potential of repurposing the FDA approved

34 disulfiram drug for its *borrelia*cidal activity. Our *in vitro* results indicate disulfiram shows

35 excellent *borrelia*cidal activity against both the log and stationary phase *B. burgdorferi*.

36 Subsequent mice studies have determined that the disulfiram eliminated *B. burgdorferi*

37 completely from hearts and urinary bladder by day 28 post infection, demonstrating the practical

38 application and efficacy of disulfiram against *B. burgdorferi in vivo*. Moreover, disulfiram

39 treated mice showed reduced expression of inflammatory markers and protected against

40 histopathology and organ damage. Furthermore, disulfiram treated mice showed significantly

41 lower amounts of total antibody titers (IgM and IgG) at day 21 and total IgG2b at day 28 post

42 infection. Mechanistically, cellular analysis of lymph nodes revealed a decrease in percentage of

43 CD19+ B cells and increase in total percentage of CD3+ T cells, CD3+ CD4+ T helpers, and

44 naïve and effector memory cells in disulfiram-treated mice. Together, we demonstrate that

45 disulfiram has the potential and could be repurposed as an effective antibiotic for treating Lyme

46 disease in near future.

47

48

49

50

Introduction

Lyme disease, a Zoonosis, is the most common reportable vector-borne disease in the United States and affects ~300,000 persons annually in North America[1], spread by the spirochete *Borrelia burgdorferi* sensu stricto (hereafter termed *B. burgdorferi or Bb*). The clinical manifestations of Lyme disease includes three phases[2]. Early infection consists of localized erythema migrans, followed within days or weeks by dissemination to the nervous system, heart, or joints in particular and subsequently resulting in persistent infections. Without antibiotics treatment, 60% of patients with Lyme disease in the United States develop arthritis, which may recur at intervals and last for months or years. Fewer patients (4 to 10%) suffer carditis, which is generally an early and nonrecurring manifestation of infection[3]. Antibiotic treatment usually with oral doxycycline, at the early localized stage of Lyme disease cures the disease in most patients[4]. However, 10 to 20 % of patients continue to experience major lingering symptoms, such as fatigue, musculoskeletal pain, and cognitive complaints, a condition known as post treatment Lyme disease syndrome (PTLDS)[5]. Several studies indicate that disseminated infection is not eradicated by conventional antibiotics such as tetracycline, doxycycline, amoxicillin or ceftriaxone in animal models tested like mice[6,7,8], dogs[9], ponies[10] and in non-human primates.[11,12] Several reports also showed that several antibiotics daptomycin and cefoperazone in combination with doxycycline or amoxicillin effectively eliminated *B. burgdorferi* persisters[13,14]. However, these antibiotic combination failed to act against *B. burgdorferi* biofilm forms[14]. Despite these findings, the PTLDS mechanisms are unclear and the plausible

71   explanations for symptoms in animal models could be *B. burgdorferi* adapting multiple immune

72   evasion mechanisms like alteration of highly immunogenic surface antigens[15,16], inhibition of

73   complement-mediated bacterial lysis[17,18] that may render antibody response ineffective, there by

74   supporting ongoing PTLDS. Therefore, based on these observations new mechanistic classes of

75   antibiotics need to be developed to treat infections raising from these resistant forms of *B.*

76   *burgdorferi.*

77   One approach to expedite the development of new antibiotics is to repurpose preexisting drugs

78   that have been approved for the treatment of other medical conditions. Previously, we screened

79   drugs (80% of them FDA approved, with a total of 4366 chemical compounds from four

80   different libraries) with high activity against the log and stationary phase of *B. burgdorferi* by

81   BacTiter-Glo™ Assay. Among them, disulfiram (Antabuse™), an oral prescription drug for the

82   treatment of alcohol abuse since 1949, was found to have the highest anti-persister activity

83   against *B. burgdorferi* [19]. In addition, disulfiram and its metabolites are potent inhibitors of

84   mitochondrial and cytosolic aldehyde dehydrogenases (ALDH)[20]. Recent U.S. clinical trials

85   using repurposed disulfiram treatments include: methamphetamine dependence (NCT00731133);

86   cocaine addiction (NCT00395850); melanoma (NCT00256230); muscle atrophy in pancreatic

87   cancer (NCT02671890); HIV infection (NCT01286259) modulator of amyloid precursor protein

88   processing (NCT03212599) and also recently initiated for previously treated Lyme disease

89   (NCT03891667)[21]. In the area of infectious disease, disulfiram has been shown have

90   antibacterial[22,23], and anti-parasitic[24] properties. Recently in a clinical setting, disulfiram appears

91   to have conferred benefit in the treatment of a limited number of patients with Lyme disease and

92   babesiosis[25]. Disulfiram is an electrophile that readily forms disulfides with thiol-bearing

93   substances. *B. burgdorferi* possess a diverse range of intracellular cofactors (e.g., coenzyme A

94   reductase)[26], metabolites (e.g., glutathione), and enzymes (e.g., thioredoxin)[27] containing

95   thiophilic residues that disulfiram can potentially modify by thiol-disulfide exchange to evoke

96   antimicrobial effects. Therefore, disulfiram has potential to inhibit *B. burgdorferi* metabolism by

97   forming mixed disulfides with metal ions[28] and it has been shown by our group previously that

98   *B. burgdorferi* require zinc and manganese as co-factors for key biological processes[29].

99   In the present study, we evaluated the antibacterial activities of disulfiram against log and

100   stationary phases of *B. burgdorferi* in more detail. Furthermore, bactericidal activity of

101   disulfiram *in vivo* was determined using the C3H/HeN mouse model of Lyme disease at early

102   onset of chronic infection i.e. day 14 and day 21 post *B. burgdorferi* infection.

103

104

105

106

107

108

109

110

111

112

113

114

115

116

117

118

119

120

121   **Results**

122   **Disulfiram as a potential antibiotic on log and stationary forms of *B. burgdorferi* B31**

123   While our initial screen of disulfiram from four drug libraries is based on Bac titer-Glo assay[19],

124   we performed our preliminary disulfiram study of varying concentrations ranging from (100 µM

125   to 0.625 µM) by Bac titer-Glo assay (Supplementary Figure 1A and 2A), which can only predict

126   the cell viability based on quantitation of ATP present, but it cannot discriminate the inhibitory

127   or bactericidal effects of the disulfiram. Further, we have performed the MICs/MBCs by gold

128   standard micro dilution assay using the morphological evaluation methods like dark field direct

129   cell counting and SYBR Green I/PI (Live/Dead) fluorescence microscopy counting in 48-well

130   plate format (Figures 1 and 2). Here, in this study we evaluated disulfiram (dissolved in both

131   DMSO and 30% hydroxypropyl β-cyclodextrin (from now on cyclodextrin) and doxycycline *in-*

132   *vitro* sensitivity of spirochete and round body morphological forms, of *B. burgdorferi* B31

133   incubated for 4-5 days with different concentrations of drugs. Appropriate concentrations of

134   cyclodextrin, DMSO and ultra-pure water in BSK medium were used as negative controls.

135   Our *in vitro* studies indicate that treatment with different concentrations ranging from 20 µM, 10

136   µM, 5 µM, 2.5 µM, 1.25 µM and 0.625 µM of disulfiram in DMSO and disulfiram in

137   cyclodextrin drugs significantly eliminated log phase spirochetes ~ 80-94% and stationary phase

138   persisters ~ 80-92% compared to the controls (Figures 1 and 2). More specifically, treatment

139   with 5 µM (1.48 µg/ml) concentration of disulfiram in DMSO and disulfiram in cyclodextrin

140   drugs significantly eliminated log phase spirochetes ~ 94% and treatment with 5 µM (1.48

141   µg/ml) concentration of disulfiram in DMSO and disulfiram in cyclodextrin drugs significantly

142   eliminated stationary phase spirochetes ~ 92% and ~ 90% respectively (Figure 2A and 2B). In

143   our study also, as reported earlier[13] doxycycline was significantly able to reduce the viability of

144   log phase *B. burgdorferi* by ~90-97% compared to the control (Fig. 1A and 1B). However,

145   doxycycline treatment had no significant effect on the cells in the stationary phase cultures as

146   observed by increasing proportion of viable cells after antibiotic exposure compared to the

147   control (Figure 2B and 2C). However, at high concentration (ranging from 50 µM-100 µM) lose

148   efficacy and shows reduced bactericidal activity with increase in concentration of disulfiram

149   drug in DMSO or cyclodextrin. These results are specific since treatment with ultra-pure water

150   or cyclodextrin or DMSO in BSK medium did not significantly reduce the viability of the

151   spirochete rich log phase culture and persisters rich stationary cultures compared to the control

152   observed in both direct dark field and SYBR Green-I /PI based fluorescent microscopy counting

153   respectively (Fig. 1A and 2A).

154   To validate our preliminary results, *B. burgdorferi* B31 log and stationary forms were further

155   evaluated *in vitro* for disulfiram in DMSO and disulfiram in cyclodextrin drugs sensitivity by a

156   fluorescent microscopy counting using SYBR Green-I (live cells stain green) and Propidium

157   Iodide (dead cells stain red). Consistently, the 5µm (1.48 µg/ml) concentration of disulfiram in

158   DMSO and disulfiram in cyclodextrin drugs significantly reduced log phase spirochetes by ~ 94

159   %, but in the remaining 6 % of the population, ~ 4 % were stained green for live while ~ 2 %

160   were stained red for dead (Figure 2B). While doxycycline significantly reduced the log phase

161   viability by ~ 97%, it did not reduce the stationary phase viability of *B. burgdorferi* (Figure 2B).

162   However, most interestingly treatment with 5 µm (1.48 µg/ml) concentration of disulfiram in

163   DMSO and disulfiram in cyclodextrin drugs significantly eliminated stationary phase spirochetes

164   ~ 92 % and ~ 90 % respectively but in the remaining 8 % and 10 %, ~ 6 % and 8 % were live

165   while ~ 2 % were dead (Figure 2B). These results agreed with the dark field microscopy

166   counting.

167   At low concentrations (ranging from 10 µM- 0.625 µM), the disulfiram in DMSO and disulfiram

168   in cyclodextrin drugs concentration response profile is sigmoid. In contrast, at higher

169   concentrations (ranging from 25 µM- 100 µM), the disulfiram drugs lose efficacy, exhibiting the

170   U-shaped or bell curve observed in the Figures 1 and 2. We attribute this loss in activity to the

171   drugs being in colloidal form. This was further analyzed by the Dynamic light scattering (DLS)

172   and Atomic force microscopy based techniques.

173   **Disulfiram forming aggregates at high concentration was shown by DLS study and AFM**

174   **based imaging**

175   Dynamic light scattering (DLS) technique was used to study the aggregation of disulfiram.

176   Supplemental figure 1 indicates a variation in the average count rate of the particles with

177   increasing concentrations of disulfiram prepared from DMSO and CD stock solutions. The

178   samples from DMSO preparation showed a linear increase in the average count rate with respect

179   to the concentration. However, the slope of the increase changed above 10 µM indicating a

180   critical aggregation concentration (CAC). The results from the CD preparation showed a non-

181   linear trend with a break at 10 µM consistent with the CAC results from DMSO preparation.

182   Atomic force microscopy-based techniques helped us to further evaluate the small volume (10

183   µL) of liquid sample aliquots and fast drying of the highly spread droplets on hydrophilic

184   substrates allow to assess the real disulfiram particle dimensions with minimal contribution of

185   secondary sample aggregation due to local increase in its concentration due to drying. In

186   supplemental figure 2 observed that very few aggregates were formed for DMSO samples for all

187   concentrations (supplemental figure 2; E-H). The smaller particles are less than 1 nm in height.

188 For cyclodextran particles, we can see larger particles that are quite wide, but also quite flat –

189 only 10 nm high, on average. These are likely particles formed due to sample drying. However,

190 for smaller particles, a crossover can be seen from 25 to 10 µM (supplemental figure 2; A-D). In

191 the former sample, we can still observe them (white arrows), but not in the latter, which is only

192 2.5 times less concentrated. Thus, this can be proof of sample aggregation, which starts to be

193 substantial only above 20 µM, as evident from our DLS data.

194 **Disulfiram treatment reduces the *B. burgdorferi* burden in tissues following dissemination**

195 **in infected C3H/HeN mice**

196 Following-up on the potent killing *in vitro* activity of disulfiram against *B. burgdorferi,* we

197 examined its efficacy *in vivo* immunocompetent C3H/HeN[30] mice and compared with

198 doxycycline. To better compare the efficacy, disulfiram (75 mg/kg of bodyweight) was

199 introduced intra peritoneally on day 14 and day 21 (to consistently develop persistent infection

200 and carditis[31]) in to post infected C3H/HeN mice at 75 mg/kg of body weight every day for 5

201 days (Figure 3A). Mice were sacrificed after 48 hours of last dose to collect tissue samples at

202 both time points (day 21 and day 28 post drug treatment). A whole ear and heart base were used

203 for cultivation and analyzing the pathogen loads. Spleen, bladder, ear and heart were collected

204 for whole-DNA extraction and Q-PCR analysis (Table 1 and Figure 3A). The *flab* gene PCR

205 positivity represent either live *Bb* or components that had not been cleared from tissues. In the

206 day 14 post disulfiram treatment group, 3 out of 5 mice were *flaB* gene PCR positive from heart,

207 bladder and ear tissues (Table1 and Figure 3B). Whereas in the doxycycline treatment (50

208 mg/kg) group, 3 out of 5 mice were positive by PCR from heart and ear tissues but none positive

209 for PCR from bladder tissues (Figure 3B). Similar results observed in cultured ear and heart

210 tissues of respective groups (data not shown). The disulfiram treatment group had statistically

211   significant lower number of *B. burgdorferi* compared to untreated infected controls (Table 2 and

212   Figure 3B). On the other hand, in the day 21 post disulfiram treatment group, 2 out of 4 mice

213   were *flaB* gene PCR positive from ear and rest of the tissues heart and bladder were PCR

214   negative (Figure 3B). Whereas in the doxycycline treatment group, 4 out of 4 mice ears were

215   PCR positive and 1 out of 4 mice bladder was PCR positive but none positive for PCR from

216   heart (Table 2 and Figure 3B). Similar results observed in cultured ear and heart tissues of

217   respective groups (data not shown). These results showed an overall better efficacy *in vivo*

218   C3H/HeN mouse to restrict the further growth and dissemination of *B. burgdorferi*.

219   **Disulfiram treatment decreases disease pathology and further reduces inflammatory**
220   **markers in the heart of *B. burgdorferi* infected C3H/HeN mice**

221   In Lyme borreliosis, heavy inflammatory infiltrates dominated by mono or polymorphonuclear

222   leukocytes are typically found at lesion sites[32]. We performed histopathology analysis of heart in

223   both the day 14 and day 21 post disulfiram treatment group mice and found normal features of

224   aorta, valves and few to no mononuclear leukocytes inflammation in the myocardium which

225   signifies inactive carditis than the infected mice (Figure 3C and supplemental figure 3), whereas

226   the doxycycline treatment group mice specifically in day 21 showed mild to moderate level of

227   mononuclear leukocytes inflammation in the aorta and valves which signifies active carditis

228   (Figure 3C and supplemental figure 3) than the infected untreated mice which showed transmural

229   infiltration of mononuclear leukocytes in the aorta and valves signifies severe active carditis

230   (Figure 3C and supplemental figure 3).

231   In infectious diseases, a hallmark of inflammatory tissue reactions is the recruitment and

232   activation of leukocytes. Chemo and cytokines play a pivotal role in mediating these events. We

233   further determined whether disulfiram treatment alters the inflammatory responses in the heart at

234　both day 14 and day 21 post infection, we evaluated *B. burgdorferi* induced myocardial

235　inflammation by quantification of mRNA transcription of CxCL1 (KC), CxCL2 (MIP-2), CCL5

236　(RANTES), TNFα, IFNγ, IL-10, IL-1β, iNOS and NOS-2 by qRT-PCR. In the day 14 post

237　disulfiram treatment group, levels of MIP-2, TNFα, IFNγ and IL-10 were significantly lower

238　(reached normal levels) relative to infected untreated mice (Figure 4). More specifically, IL-10

239　levels were reduced to 60-fold (Figure 4C), while MIP-2, TNFα, and IFNγ reduced to 10-fold

240　(Figures 4 A, D&E). There was no change in NOS2 and iNOS levels (Figures 4 G&H). On the

241　other hand, in the day 21 post disulfiram treatment group, levels of MIP-2, RANTES, TNFα,

242　IFNγ, IL-1β, and IL-10 were significantly lower (touched to normal levels) relative to infected

243　untreated mice (Figure 4), while iNOS and NOS-2 levels were significantly higher relative to

244　infected untreated mice (Figure 4 G&H). More specifically, IL-10 levels were reduced to 100-

245　fold (Figure 4 C), and other cytokines like MIP-2, TNFα, IL-1β, and IFNγ levels were reduced

246　ten to sixty-fold (Figures 4 A, D, F&E). While NOS-2 and iNOS, which have role in immune

247　regulation and tissues remodeling, were significantly higher compared to infected untreated mice

248　(Figures 4 G & H). These results indicate that disulfiram affects the regulation and/or balance of

249　Th1 (MIP-2, RANTES, TNFα, IFNγ and IL-1β), Th2 (IL-10) and protective Macrophage M1

250　(NOS2, iNOS) responses to *B. burgdorferi* at day 21 and day 28 post infection. However,

251　doxycycline treatment group have only reduced few cytokines like IL-10, TNFα, and IFNγ at

252　day 14 and 21 post treatment (Figures 4 C, D, & E). While NOS-2 levels elevated at day 21 and

253　MIP-2 levels reduced at day 28 post infection (Figures 4 G & H).

254　**Disulfiram treatment reduces antibody titers in the *B. burgdorferi* infected mouse**

255　We next sought to determine whether disulfiram treatment affects antibody development during

256　day 14 and day 21 post *B. burgdorferi* infection, we measured the serum levels of each subtype

257   of total immunoglobulins using an ELISA. The results at day 21, showed that the total amount of

258   IgM and IgG levels were significantly lower in disulfiram treated mice compared infected

259   control mice (Figure 5A). Among the IgG subtypes, total IgG1 levels were significantly lower

260   than the infected control mice (Figure 5A). However, there was no effect on other IgG subtypes

261   like IgG2a, IgG2b and IgG3 (Figure 5A). While at day 28, only trend towards lower IgG levels

262   observed but were not statistically significant (Figure 5B). However, IgG2b levels were

263   significantly lower in disulfiram treated mice and no effect on other IgG subtypes like IgG1,

264   IgG2a and IgG3 (Figure 5B). Whereas doxycycline treatment group does not show any reduction

265   of antibody titers at day 21 and day 28 respectively (Figures 5A & B). These data suggest that

266   the disulfiram treatment might induced development of antibody subtypes very efficiently and

267   affect IgG class switching, which may represent a contributing factor in lowering *B. burgdorferi*

268   titers at day 21 and clearance of *Bb* more efficiently at day 28. However, we cannot exclude the

269   fact that there is a possibility that B cells expressing different immunoglobulin isotypes are

270   selectively expanded.

271   **Disulfiram reduces lymphoadenopathy in *B. burgdorferi* infected C3H/HeN mice**

272   Lymphadenopathy, a hall mark of acute Lyme borreliosis[33] manifestation is characterized by

273   increased cellularity and the accumulation of large pleomorphic IgM- and IgG- positive plasma

274   cells. To determine whether disulfiram treatment reduces the lymph node enlargement, at day 28

275   we collected peripheral (axillary, brachial, cervical and inguinal) lymphnodes (pLNs) and

276   determine the cell number counts followed by analyzing B and T cell populations by flow

277   cytometry. In disulfiram treatment mice, total lymphocytes of pLNs were statistically reduced in

278   comparison to infected control mice (Figure 6). Doxycycline treatment mice also shown similar

279   result. Further, our pLNs FACS analysis of disulfiram treatment mice had significant decrease of

280   the percentages of CD19+ B cells, and significant increase of the percentages of CD3+ T cells in

281   comparison to infected control mice (Figure 6). Further among the CD3+ subsets, CD3+ CD4+

282   helper T cells and CD3+ CD8+ cytotoxic T cells were not affected in comparison to infected

283   control mice (Figure 6). However, when we compare naïve uninfected mice with all three

284   infected groups (infected PBS treated, infected doxycycline treated and disulfiram treated)

285   showed significant decrease of the percentages of CD3+ CD8+ cytotoxic T cells (Figure 6), and

286   significant increase of the percentages of CD3+ CD4+ helper T cells (Figure 6). Another

287   hallmark of effective and long-term protection is the generation of memory T cells. They provide

288   an efficient immune response on pathogen re-exposure[34]. We further analyzed CD4$^+$ T helper

289   subsets by labeling naïve (CD62L$^+$), early effector (CD62L$^-$/CD44$^-$), effector (CD44$^+$) and

290   memory T cells (CD62L$^+$/CD44$^+$). Analysis of helper T cells in comparison to naïve uninfected

291   mice revealed that disulfiram treatment mice led to a significant increase of early

292   effector/effector and memory T cells and to a significant decrease of naïve T cells in pLNs

293   (Figure 6). Similar trend was observed in infected PBS treated and infected doxycycline treated

294   mice (Figure 6).

295   **Discussion**

296   Since antibiotics are the top-of-the-line options to treat infections, there remains a dire need and

297   a practical approach to bring more efficient antibiotics to clinic. The repurposing of FDA

298   approved antibiotics through fast-track approvals can be an excellent solution. In this current

299   study, we evaluated the borreliacidal potential of FDA approved drug disulfiram *in vitro* and *in*

300   *vivo* based on our previous high-throughput screening hits[19,35]. We performed preliminary *in*

301   *vitro* antimicrobial assays by Bac-titer glo assay with wide range of disulfiram concentrations

302   (0.625 µM to 100 µM). Later, we confirmed the preliminary results by comparing antimicrobial

303   effect of disulfiram to doxycycline and used most reliable quantitative methods performed to

304   establish the bactericidal activity[36,37]. Disulfiram in both soluble forms (DMSO or cyclodextrin)

305   inhibited the the growth of *B. burgdorferi* strain B31 at an MIC^{90} range of 0.74 to 2.97 µg/ml in

306   case of log phase cultures (~94%) and stationary phase cultures (~90%) at 1.48 µg/ml,

307   respectively (Figures 1 and 2), and with MBC varying from 1.48 µg/ml to 2.97 µg/ml for log

308   and stationary phase cultures. The immediate deceleration in log and stationary phases of *B.*

309   *burgdorferi* growth on low dose of disulfiram treatment is attributed to the rapid cleavage of

310   disulfiram by thiophilic residues in intracellular cofactors like coenzyme A reductase[26], enzymes

311   like thioredoxin[27], metal ions like zinc and manganese[29], and cofactors of *B. burgdorferi*, which

312   are hypothesized to instigate an abrupt halt in *B. burgdorferi* metabolism, thus evokes killing of

313   *B. burgdorferi*. A similar mechanism of action is proposed for pathogens like Giardia, Bacillus,

314   drug resistant Mycobacterium, and multidrug resistant Staphylococcus [38,22,23,39,40].

315   Disulfiram is an oral medication that is approved by the U.S. Food and Drug Administration

316   (FDA) for administration of up to 500 mg daily[41]. Pharmacokinetic studies in humans has shown

317   that disulfiram has a half-life ($t_{1/2}$) of 7.3 h and a mean plasma concentration of 1.3 nM, although

318   significant intersubjective variations are noted[42]. The toxicity of both disulfiram and its

319   metabolites have also been broadly investigated in cell and animal studies, which yielded no

320   evidence for teratogenic, mutagenic, or carcinogenic effects[43]. DMSO proved to be low dose

321   toxic *in vivo*[44] so, we have used non-toxic cyclodextrin[45,46] as a solubilizing agent for

322   disulfiram *in vivo* studies. Based on these observations, we conducted our preliminary *in vivo*

323   mouse efficacy studies by administering (I.P) low dose of 10 mg/kg of body weight disulfiram to

324   infected C3H/HeN mice for 5 days and found that these mice could not able to clear the *B.*

325   *burgdorferi* from tissues (unpublished data). However as shown in the current study, when we

326   repeated *in vivo* C3H/HeN mouse efficacy studies by administering (I.P) 75 mg/kg of body

327   weight disulfiram to infected mice for 5 days, all infected mice either reduced or cleared the

328   bacteria in most of the tissues at 21 and 28 post infection (Tables 1, 2 and Figure 3). C3H mice

329   develop bradycardia and tachycardia beginning on day 7 through 60 days after *B. burgdorferi*

330   inoculation and reaches severe inflammation particularly in C3H mice on day 15 to 21 post

331   infection[31]. So, we have chosen C3H/HeN mouse model for our efficacy studies and day 14 or

332   day 21 post infection as time points for antibiotics treatments. Lyme carditis, a macrophage-

333   mediated pathology not directly influenced by *B. burgdorferi* specific antibodies, but by

334   inflammatory micro environment created by mRNAs for proinflammatory Th1 cytokines (IL-1β,

335   TNF-α, and IFN-γ), Th2 (IL-10), and other M1/M2 protective macrophage polarizing factors like

336   iNOS and NOS2 derived from macrophages and T cells[47,48,49]. Similarly, chemokines like MIP-2

337   (macrophage inflammatory protein 2), KC, and RANTES (regulated upon activation, normal T

338   cell expressed and secreted) preferentially attract monocytes and lymphocytes significantly

339   contributing to the inflammation and tissue damage in Lyme disease[50]. We have shown that in

340   disulfiram treatment mice there is a significant reduction in the infiltration of leucocytes in the

341   heart wall and leads to no inflammation (inactive carditis) compared to doxycycline treated

342   group (active mild carditis) and PBS infected group (active severe carditis) at day 21 or day 28

343   post infection (Figure 3). Which implies that disulfiram treatment reduced the inflammatory

344   microenvironment by reducing the inflammatory chemokines (MIP-2 and RANTES), and

345   cytokines (IL-10, IL-1β, TNF-α, and IFN-γ) and further reduces the disease severity in heart.

346   Macrophage phenotype is flexible, and once the infection is cleared and a more anti-

347   inflammatory environment is created, these inflammatory cells may switch to a proresolution M2

348   phenotype[51]. Henceforth, in disulfiram treated mice since infection is cleared, M2 polarizing

349   factors like NOS2 (iNOS) were elevated than the doxycycline treated group and PBS infected

350   group at day 21 or day 28 post infection (Figure 4). However, underlying mechanism involved in

351   differential expression of chemo and cytokines and their effect on disease severity needs to be

352   investigated.

353   Further, in this study we found lower bacterial burden in ear, heart and bladder of disulfiram

354   treated mice compared to PBS treated infected mice at 21 days post infection (Figure 5),

355   indicating that the disulfiram administration might have promoted the antibody mediated killing

356   early in the infection, thus not only limit *B. burgdorferi* colonization in tissues but also altered

357   the development of adaptive immune response, which may reduce the tissue inflammation as

358   observed in heart[52,53]. In fact, *B. burgdorferi* infection leads to strong and sustained IgM

359   response and delayed development of long-lived antibody and B cell memory[54]. So, disulfiram

360   treated mice might have accelerated long lived antibody and B cell memory development, which

361   resulted in statistically lower amount of total IgM, IgG and IgG1 in day 21 post infection (Figure

362   5). On the other hand later at day28 post infection, disulfiram treated mice have higher amounts

363   of total IgM, IgG1 and IgG3isotypes, which all bind to C1q and activate the classical pathway,

364   whereas IgG2a and IgG2b bind to the Fc receptor[55]. As such, it is likely possible that those

365   immuno-complexes formed with C1q-binding antibodies cannot be opsonized by the

366   complement system during infection due to the absence of C1q thus fail to be engulfed by

367   phagocytes and accumulated within the circulation system. Lymphoadenopathy observed during

368   Lyme borrreliosis is caused by a massive increase in lymph node cellularity triggered by the

369   accumulation of live *B. burgdorferi* spirochetes into the lymph nodes. This increase in cellularity

370   is due to accumulation of CD19+ B cells[33]. Disulfiram treatment not only alleviates

371   lymphoadenopathy but also reduces the percentage of CD19+ B cells in day 28 post infected

372   mice (Figure 6). An important function of CD4+ T cells is their ability to enhance antibody-

373   mediated immunity by driving affinity maturation and the development of long-lived plasma

374   cells and memory B cells. However, it appears unlikely that the protective B cell response to *B.*

375   *burgdorferi*, a highly complex pathogen expressing many immunogenic surface antigens, is

376   confined to T-independent antibody responses alone. Even though, disulfiram treated mice

377   induces increase in percentage of CD3+ CD4+, Naïve, effector and memory T cells, further

378   studies are needed to understand the role of these increased T cells in disease resolution and

379   bacteria clearance.

380   In summary, the disulfiram drug not only successfully cleared the bacteria but also reduced the

381   inflammation in heart tissue in C3H/HeN mice at day 28 post infection. Furthermore, disulfiram

382   reduced antibody titers followed by nullifying lymphoadenopathy. The preclinical data offered

383   here is beneficial in ascertaining the effectiveness of disulfiram and aids in future mechanistic

384   and translation research studies. Moreover, the disulfiram can exploit multiple mechanisms to

385   show its inhibitory effects both *in vitro* and *in vivo*. Although the results from our *in vivo* study

386   cannot be extrapolated directly to clinical practice, they form strong basis for future follow-up

387   studies, and promote the development of effective formulations of disulfiram for clinical

388   management of Lyme disease.

389   **Materials and Methods**

390   **Culturing and growth conditions of *B. burgdorferi* B31**

391   *Borrelia burgdorferi sensu stricto* low passage strain B31 was (obtained from the American

392   Type Culture Collection Manassas, VA) used for MIC tests and all infection studies in C3H/HeN

393   mice. Bacteria cultures were started by thawing -80^{0}C glycerol stocks of *B. burgdorferi* (titer,

394   ~10^7 CFU/ml) and diluting 1:40 into fresh Barbour-Stoner-Kelly (BSK) complete medium with

395   6% rabbit serum followed by incubating at 33^0C. After incubation for 4-5 days log phase, and 8-

396   9 days stationary-phase *B. burgdorferi* culture (~10^6 borrelia/mL) was transferred into a 48-well

397   plate for evaluation with the drugs.

Drug formulations

399   The disulfiram (Sigma, USA) stock solution (50 mM) was made by dissolving in sterile 30%

400   hydroxypropyl β-cyclodextrin (Sigma) and also another disulfiram stock solution (20 mM) was

401   made by dissolving in sterile 100 % DMSO (Tocaris bioscience, UK). A stock solution of 100

402   mM of doxycycline (as a positive control) was made by dissolving the doxycycline powder in

403   ultra-pure MilliQ water. All drug stocks were passed through 0.22 μm filters (Millipore-Sigma),

404   used within 72 h of preparation and were not subject to freezing temperatures. Working solutions

405   was made by mixing desired volume of stock solutions in desired volume of ultra-pure MilliQ

406   water. Further, the vehicle for hydroxypropyl β-cyclodextrin (cyclodextrin) and DMSO controls

407   were made similarly and it is important to note that the vehicle controls were identical to the test

408   formulation in every single aspect except for the active ingredient. This measure was strictly

409   followed for vehicle control wherever used in entire study.

In-vitro testing of antibiotics by BacTiter Glo® assay, microdilution and SYBR Green I/PI

assay methods

412   The MIC was determined by using Bac Titer-Glo microbial cell viability assay[29]. After 72 hours,

413   100 μL of culture was taken from each well and mixed with 100 μL of Bac Titer-Glo® reagent

414   (Promega, Madison, WI, USA). Then, the assay was performed according to the manufacturer's

415   instructions. Luminescence was measured on a CLARIOstar micro plate reader at an integration

416   time of 500 milliseconds.

417   A standard microdilution method was used to determine the minimum inhibitory concentration

418   (MIC) of the antibiotics tested[56]. Approximately, 1×10^6 *B. burgdorferi* were inoculated into

419   each well of a 48-well tissue culture microplate containing 900 μL of BSK medium per well. The

420   cultures were then treated with 100 μL of each drug at varying concentrations ranging from

421   0.625, 1.25, 2.5, 5, 10 and 20 μM. Control cultures were treated with respective vehicles, and all

422   experiments were run in triplicate. The well plate was covered with parafilm and placed in the

423   33^0C incubator with 5% CO_2 for 4 days. Spirochetes proliferation was assessed using a bacterial

424   counting chamber (Petroff-Hausser Counter) after the 4-5 days incubation followed by dark-field

425   and fluorescence microscopy. To further determine the minimum bactericidal concentration

426   (MBC) of the antibiotics tested (the minimum concentration beyond which no spirochetes can be

427   sub cultured after a 3-week incubation period), wells of a 48-well plate were filled with 1 mL of

428   BSK medium and 20 μL of antibiotic-treated spirochetes were added into each of the wells. The

429   well plate was wrapped with parafilm and placed in the 33^0C incubator with 5 % CO_2 for 3

430   weeks (21 days). After the incubation period, the plate was removed and observed for motile

431   spirochetes in the culture by dark-field and further cell proliferation was assessed using the

432   SYBR Green I/PI assay fluorescence microscopy. All these experiments were repeated at least

433   three times. Statistical analyses were performed using Student's t -test.

434   **Dynamic light scattering**

435   The stock solutions of 1M disulfiram was prepared either in DMSO or in 30% (w/v)

436   hydroxypropyl ß-cyclodextrin (CD). Disulfiram was then diluted in bovine serum albumin

437   (BSA) solution to obtain disulfiram concentration 0.125 μM, 0.25, 0.5, 10, 25, 50, and 100 μM,

438   and 5% (w/v) BSA in the final solution for DLS. The measurements were obtained from

439   Brookhaven 90-Plus particle size analyzer (Brookhaven instruments corporation) at an angle of

440   90° with 10% dust cutoff filter. The results represent average of three measurements.

441   **Atomic force microscopy**

442   Atomic force microscopy (AFM) samples have been prepared from drugs disulfiram-CD and

443   disulfiram-DMSO solutions of respective concentrations (100 μM, 25 μM, 10 μM and 5 μM) on

444   clean silicon wafers that were plasma-treated to increase hydrophilicity. 10 µL droplets were

445   deposited, spreading for most of the surface of 1 cm^2 wafers and were quickly dried in a

446   desiccator under vacuum to minimize additional aggregation due to local increase in

447   concentrations. AFM imaging has been performed with NX-10 AFM (Park Systems, Korea)

448   operating in non-contact mode with Micromasch NCS15 AL BS tips (NanoandMore, USA) at

449   0.8 Hz with 256 pixels per line.

450   *In vivo* **testing of drugs in immunocompetent C3H/HeN mice**

451   Four weeks old female C3H/HeN mice, were purchased from Charles River Laboratories,

452   Wilmington, Massachusetts. All mice were maintained in the pathogen-free animal facility

453   according to animal safety protocol guidelines at Stanford University under the protocol ID

454   APLAC-30105.   All experiments were in accordance with protocols approved by the

455   Institutional Animal Care and Use Committee of Stanford University. The mice (5 week) were

456   infected subcutaneously close behind the neck with 0.1 mL BSK medium containing log phase

457   10^5 *B. burgdorferi* B31. For *in vivo* studies, we have used only disulfiram soluble in

458   cyclodextrin. On the 14 and 21 days post Bb infection, the mice were intraperitoneally

459   administered a daily dose of drugs, disulfiram (75 mg/kg) and doxycycline (50 mg/kg) for 5

460   consecutive days (Figure 3A). After 48 hours of the last dose of administering compounds, both

461   groups (day 21 and day 28 post Bb infection) of mice were terminated and their urinary bladders,

462 ears, and hearts were collected. The DNA was extracted from urinary bladder, ear and heart. The

463 absence of *B. burgdorferi* marked the effectiveness of the treatment in these organisms.

464 Quantification of important pro/anti-inflammatory immune marker transcripts and

465 histopathology of heart was also done. At termination on day 28 post infection, spleen and

466 peripheral lymph nodes (axillary, brachial, cervical and inguinal) were also collected for

467 immunophenotyping.

468 **Quantitative (Q-PCR) and Real-time PCR (RT-PCR) analysis**

469 Urinary bladder, ear punches, heart bases were homogenized and DNA was extracted using the

470 NucleoSpin tissue kit according to the manufacturer's instructions (Düren, Germany). Q-PCR

471 from above tissues were performed in blinded samples using *B. burgdorferi* Fla-B gene specific

472 primers and a probe. These primers were listed as follows: Fla-B primers Flab1F 5'-

473 GCAGCTAATGTTGCAAATCTTTTC-3', Flab1R 5'-GCAGGTGCTGGCTGTTGA-3' and

474 TAMRA Probe 5'-AAACTGCTCAGGCTGCACCGGTTC-3' according to the published

475 protocol. Reactions were performed in duplicate for each sample. Results were plotted as the

476 number of Fla B copies per microgram of tissue. The lower limit of detection was 10 to 100

477 copies of *B. burgdorferi* Fla-B DNA per mg of tissue. In addition to standard laboratory

478 measures to prevent contamination, negative controls (containing PCR mix, Fla-B primers,

479 probe, and Taq polymerase devoid of test DNA) were included.

480 Total RNA was extracted from tissues using RNeasy mini kit (Qiagen, USA) and reverse

481 transcribed using a high-capacity cDNA reverse transcription kit (Invitrogen, USA). cDNA was

482 subjected to real-time PCR using primer and TAMRA probes (Stanford Protein and Nucleic acid

483 Facility) previously described[57]. PCR data are reported as the relative increase in mRNA

484   transcript levels of CxCL1 (KC), CxCL2 (MIP-2), CCL5 (RANTES), IL-10, TNF-α, IFN-γ,

485   iNOS and NOS2 normalized to respective levels of GAPDH.

486   **Histopathology**

487   For histopathology, heart samples were fixed in 10% formalin buffer followed by staining of

488   vertical histological sections with hematoxylin and eosin dye. Heart tissues were assessed for

489   inflammation by microscopic examination at intermediate (10X), and high (40X)-power

490   magnification and were scored for severity of inflammation (carditis, vasculitis) according to the

491   percentage of inflammation at the heart base upon examination at low power (10X). Scores of 0

492   (none), 1 (minimal; less than 5%), 2 (mild; between 5% and 20%), 3 (moderate; between 20%

493   and 35%), 4 (marked; between 35% and 50%), and 5 (severe; greater than 50%) were assigned

494   for the severity of inflammation[58,31]. Myocarditis consisted of focal or diffuse interstitial

495   infiltrates of mononuclear leukocytes in the myocardium. The microscopic photographs were

496   captured on Olympus CX-41 microscope (Olympus, Tokyo, Japan). The images are shown at

497   10X and 40X magnification

498   **Quantification of total Immunoglobulins in serum by ELISA**

499   Quantification of total mouse immunoglobulin concentration IgA, IgM, IgG, IgG1, IgG2a,

500   IgG2b, and IgG3 in mouse serum was done using Ready-Set-Go ELISA kits (Invitrogen, USA).

501   **Flow cytometry**

502   Single cell suspensions of lymphoid tissues were prepared as described[57], live/dead cell viability

503   stain was used to eliminate dead cells followed by single cells separation from doublets by FSC-

504   A vs FSC-H plots. Cells were incubated in Fc blocking for 15 min at 4°C in staining buffer and

505   incubated with the appropriate marker for surface staining in the dark for 30 min at 4°C. Surface

506   lineage markers for T cells CD3, CD4, CD8, CD62L, CD44 and B cells was CD-19 conjugated

507   with PercP Cy5.5 (Tonbo Biosciences) were described previously[57]. Cells were acquired on a

508   BD-LSR II flow cytometer and data analyzed using Flow Jo software.

509   **Statistics**

510   Data analysis was done using Graph Pad Prism software. Single comparisons within uninfected

511   or drug treated groups and infected groups were analyzed with two-tailed paired t-test, with

512   unpaired t-test with Welch's correction and with multiple t-tests. $\alpha = 0.05$ for all tests. *$p < 0.05$,

513   ** $p < 0.01$, *** $p < 0.001$, ****$p < 0.0001$.

514

515

516

517   **References**

518   1.   CDC. *TICKBORNE DISEASES OF THE UNITED STATES A Reference Manual for*
519   *Healthcare Providers*.

520   2.   Steere, A. C. Lyme Disease. *N. Engl. J. Med.* **345**, 115–125 (2001).

521   3.   STEERE, A. C. *et al.* Lyme Carditis: Cardiac Abnormalities of Lyme Disease. *Ann.*
522   *Intern. Med.* **93**, 8 (1980).

523   4.   Nadelman, R. B. *et al.* Prophylaxis with Single-Dose Doxycycline for the Prevention of
524   Lyme Disease after an *Ixodes scapularis* Tick Bite. *N. Engl. J. Med.* **345**, 79–84 (2001).

525   5.   Aucott, J. N. Posttreatment Lyme Disease Syndrome INTRODUCTION: NATURE OF
526   THE PROBLEM. doi:10.1016/j.idc.2015.02.012

527   6.   Hodzic, E., Feng, S., Holden, K., Freet, K. J. & Barthold, S. W. Persistence of Borrelia
528   burgdorferi following antibiotic treatment in mice. *Antimicrob. Agents Chemother.* **52**,
529   1728–36 (2008).

530   7.   Hodzic, E., Imai, D., Feng, S. & Barthold, S. W. Resurgence of Persisting Non-Cultivable
531   Borrelia burgdorferi following Antibiotic Treatment in Mice. *PLoS One* **9**, e86907 (2014).

532   8.   Barthold, S. W. *et al.* Ineffectiveness of tigecycline against persistent Borrelia burgdorferi.
533   *Antimicrob. Agents Chemother.* **54**, 643–51 (2010).

534 9.   Straubinger, R. K., Summers, B. A., Chang, Y. F. & Appel, M. J. Persistence of Borrelia
535   burgdorferi in experimentally infected dogs after antibiotic treatment. *J. Clin. Microbiol.*
536   **35**, 111–6 (1997).

537 10. Chang, Y.-F. *et al.* Antibiotic treatment of experimentally Borrelia burgdorferi-infected
538   ponies. *Vet. Microbiol.* **107**, 285–294 (2005).

539 11. Embers, M. E. *et al.* Persistence of Borrelia burgdorferi in Rhesus Macaques following
540   Antibiotic Treatment of Disseminated Infection. *PLoS One* **7**, e29914 (2012).

541 12. Crossland, N. A., Alvarez, X. & Embers, M. E. Late Disseminated Lyme Disease:
542   Associated Pathology and Spirochete Persistence Posttreatment in Rhesus Macaques. *Am.*
543   *J. Pathol.* **188**, 672–682 (2018).

544 13. Feng, J., Auwaerter, P. G. & Zhang, Y. Drug Combinations against Borrelia burgdorferi
545   Persisters In Vitro: Eradication Achieved by Using Daptomycin, Cefoperazone and
546   Doxycycline. *PLoS One* **10**, e0117207 (2015).

547 14. Feng, J., Weitner, M., Shi, W., Zhang, S. & Zhang, Y. Eradication of Biofilm-Like
548   Microcolony Structures of Borrelia burgdorferi by Daunomycin and Daptomycin but not
549   Mitomycin C in Combination with Doxycycline and Cefuroxime. *Front. Microbiol.* **7**, 62
550   (2016).

551 15. Kenedy, M. R., Lenhart, T. R. & Akins, D. R. The role of Borrelia burgdorferi outer
552   surface proteins. *FEMS Immunol. Med. Microbiol.* **66**, 1–19 (2012).

553 16. Rogovskyy, A. S. & Bankhead, T. Variable VlsE is critical for host reinfection by the
554   Lyme disease spirochete. *PLoS One* **8**, e61226 (2013).

555 17. Kung, F., Anguita, J. & Pal, U. Borrelia burgdorferi and tick proteins supporting pathogen
556   persistence in the vector. *Future Microbiol.* **8**, 41–56 (2013).

557 18. de Taeye, S. W., Kreuk, L., van Dam, A. P., Hovius, J. W. & Schuijt, T. J. Complement
558   evasion by Borrelia burgdorferi: it takes three to tango. *Trends Parasitol.* **29**, 119–128
559   (2013).

560 19. Pothineni, V. *et al.* Identification of new drug candidates against Borrelia burgdorferi
561   using high-throughput screening. *Drug Des. Devel. Ther.* **10**, 1307 (2016).

562 20. Jennifer P. Lam, ‡, Dennis C. Mays, ‡ and & James J. Lipsky*, ‡,§. Inhibition of
563   Recombinant Human Mitochondrial and Cytosolic Aldehyde Dehydrogenases by Two
564   Candidates for the Active Metabolites of Disulfiram†. (1997). doi:10.1021/BI970948E

565 21. ClinicalTrials.gov. Bethesda (MD): National Library of Medicine (US); 2019 Jul 14.
566   Available at:
567   https://clinicaltrials.gov/ct2/results?cond=&term=disulfiram&cntry=&state=&city=&dist=
568   . (Accessed: 9th July 2019)

569 22. Long, T. E. Repurposing Thiram and Disulfiram as Antibacterial Agents for Multidrug-
570   Resistant Staphylococcus aureus Infections. *Antimicrob. Agents Chemother.* **61**, e00898-
571   17 (2017).

572 23. Horita, Y. *et al.* Antitubercular activity of disulfiram, an antialcoholism drug, against
573   multidrug- and extensively drug-resistant Mycobacterium tuberculosis isolates.

574   *Antimicrob. Agents Chemother.* **56**, 4140–5 (2012).

575   24.   Galkin, A. *et al.* Structural basis for inactivation of Giardia lamblia carbamate kinase by
576   disulfiram. *J. Biol. Chem.* **289**, 10502–9 (2014).

577   25.   Liegner, K. B., Liegner & B., K. Disulfiram (Tetraethylthiuram Disulfide) in the
578   Treatment of Lyme Disease and Babesiosis: Report of Experience in Three Cases.
579   *Antibiotics* **8**, 72 (2019).

580   26.   Boylan, J. A. *et al. Borrelia burgdorferi bb0728* encodes a coenzyme A disulphide
581   reductase whose function suggests a role in intracellular redox and the oxidative stress
582   response. *Mol. Microbiol.* **59**, 475–486 (2006).

583   27.   Parsonage, D. *et al.* Broad specificity AhpC-like peroxiredoxin and its thioredoxin
584   reductant in the sparse antioxidant defense system of Treponema pallidum. *Proc. Natl.*
585   *Acad. Sci. U. S. A.* **107**, 6240–5 (2010).

586   28.   Barth, K. & Malcolm, R. Disulfiram: An Old Therapeutic with New Applications. *CNS*
587   *Neurol. Disord. - Drug Targets* **9**, 5–12 (2010).

588   29.   Pothineni, V. raveendra *et al.* Borreliacidal activity of Borrelia metal transporter A
589   (BmtA) binding small molecules by manganese transport inhibition. *Drug Des. Devel.*
590   *Ther.* **9**, 805 (2015).

591   30.   Barthold, S. W., Beck, D. S., Hansen, G. M., Terwilliger, G. A. & Moody, K. D. *Lyme*
592   *Borreliosis in Selected Strains and Ages of Laboratory Mice*. (1990).

593   31.   Armstrong, A. L., Barthold, S. W., Persing, @r', D. H. & Beck, D. S. *CARDITIS IN*
594   *LYME DISEASE SUSCEPTIBLE AND RESISTANT STRAINS OF LABORATORY MICE*
595   *INFECTED WITH BORRELIA BURGDORFERJ. Am. J. Trop. Med. Hyg* **47**, (1992).

596   32.   Sigal, L. H. LYME DISEASE:A Review of Aspects of Its Immunology and
597   Immunopathogenesis. *Annu. Rev. Immunol.* **15**, 63–92 (1997).

598   33.   Tunev, S. S. *et al.* Lymphoadenopathy during Lyme Borreliosis Is Caused by Spirochete
599   Migration-Induced Specific B Cell Activation. *PLoS Pathog.* **7**, e1002066 (2011).

600   34.   Gourley, T. S., Wherry, E. J., Masopust, D. & Ahmed, R. Generation and maintenance of
601   immunological memory. *Semin. Immunol.* **16**, 323–333 (2004).

602   35.   Pothineni, V. R. *et al.* Screening of NCI-DTP library to identify new drug candidates for
603   Borrelia burgdorferi. *J. Antibiot. (Tokyo).* **70**, 308–312 (2017).

604   36.   Sapi, E. *et al.* Evaluation of in-vitro antibiotic susceptibility of different morphological
605   forms of Borrelia burgdorferi. *Infect. Drug Resist.* **4**, 97–113 (2011).

606   37.   Feng, J., Wang, T., Zhang, S., Shi, W. & Zhang, Y. An Optimized SYBR Green I/PI
607   Assay for Rapid Viability Assessment and Antibiotic Susceptibility Testing for Borrelia
608   burgdorferi. *PLoS One* **9**, 111809 (2014).

609   38.   Borlinghaus, J. *et al.* Allicin: Chemistry and Biological Properties. *Molecules* **19**, 12591–
610   12618 (2014).

611   39.   Galkin, A. *et al.* Structural Basis for Inactivation of *Giardia lamblia* Carbamate Kinase by
612   Disulfiram. *J. Biol. Chem.* **289**, 10502–10509 (2014).

613 40. Frazier, K. R., Moore, J. A. & Long, T. E. Antibacterial activity of disulfiram and its
614   metabolites. *J. Appl. Microbiol.* **126**, 79–86 (2019).

615 41. Wright, C. & Moore, R. D. Disulfiram treatment of alcoholism. *Am. J. Med.* **88**, 647–655
616   (1990).

617 42. Johansson, B. A review of the pharmacokinetics and pharmacodynamics of disulfiram and
618   its metabolites. *Acta Psychiatr. Scand. Suppl.* **369**, 15–26 (1992).

619 43. Benjamin, E. M. Peter K. Gessner and Teresa Gessner Disulfiram and its Metabolite
620   Diethyldithiocarbamate. Pharmacology and Status in the Treatment of Alcoholism, HIV
621   Infection, AIDS and Heavy Metal Toxicity Chapman & Hall, London, 1992; 452 pp.,
622   £75.00. *J. Appl. Toxicol.* **13**, 306–306 (1993).

623 44. Galvao, J. *et al.* Unexpected low-dose toxicity of the universal solvent DMSO. *FASEB J.*
624   **28**, 1317–1330 (2014).

625 45. De Schaepdrijver, L. *et al.* Juvenile animal testing of hydroxypropyl-β-cyclodextrin in
626   support of pediatric drug development. *Reprod. Toxicol.* **56**, 87–96 (2015).

627 46. Li, P. *et al.* Comparison in toxicity and solubilizing capacity of hydroxypropyl-β-
628   cyclodextrin with different degree of substitution. *Int. J. Pharm.* **513**, 347–356 (2016).

629 47. Doyle, M. K. *et al.* Cytokines in Murine Lyme Carditis: Th1 Cytokine Expression Follows
630   Expression of Proinflammatory Cytokines in a Susceptible Mouse Strain. *J. Infect. Dis.*
631   **177**, 242–246 (1998).

632 48. Lasky, C. E., Olson, R. M. & Brown, C. R. Macrophage Polarization during Murine Lyme
633   Borreliosis. *Infect. Immun.* **83**, 2627–2635 (2015).

634 49. Zhi, H., Xie, J. & Skare, J. T. The Classical Complement Pathway Is Required to Control
635   Borrelia burgdorferi Levels During Experimental Infection. *Front. Immunol.* **9**, 959
636   (2018).

637 50. Sprenger, H. *et al. Borrelia burgdorferi Induces Chemokines in Human Monocytes.*
638   *INFECTION AND IMMUNITY* **65**, (1997).

639 51. Davis, M. J. *et al.* Macrophage M1/M2 polarization dynamically adapts to changes in
640   cytokine microenvironments in Cryptococcus neoformans infection. *MBio* **4**, e00264-13
641   (2013).

642 52. LaRocca, T. J. *et al.* The bactericidal effect of a complement-independent antibody is
643   osmolytic and specific to Borrelia. *Proc. Natl. Acad. Sci. U. S. A.* **106**, 10752–7 (2009).

644 53. Katona, L. I., Ayalew, S., Coleman, J. L. & Benach, J. L. A bactericidal monoclonal
645   antibody elicits a change in its antigen, OspB of Borrelia burgdorferi, that can be detected
646   by limited proteolysis. *J. Immunol.* **164**, 1425–31 (2000).

647 54. Hastey, C. J., Elsner, R. A., Barthold, S. W. & Baumgarth, N. Delays and diversions mark
648   the development of B cell responses to Borrelia burgdorferi infection. *J. Immunol.* **188**,
649   5612–22 (2012).

650 55. Sörman, A., Zhang, L., Ding, Z. & Heyman, B. How antibodies use complement to
651   regulate antibody responses. *Mol. Immunol.* **61**, 79–88 (2014).

652 56. Dever, L. L., Jorgensen, J. H. & Barbour3, A. G. *In Vitro Antimicrobial Susceptibility*

653   *Testing of Borrelia burgdorferi: a Microdilution MIC Method and Time-Kill Studies.*
654   *JOURNAL OF CLINICAL MICROBIOLOGY* **30**, (1992).

655 57.   Potula, H.-H., Richer, L., Werts, C. & Gomes-Solecki, M. Pre-treatment with
656   Lactobacillus plantarum prevents severe pathogenesis in mice infected with Leptospira
657   interrogans and may be associated with recruitment of myeloid cells. *PLoS Negl. Trop.*
658   *Dis.* **11**, e0005870 (2017).

659 58.   Montgomery, R. R. *et al.* Recruitment of macrophages and polymorphonuclear leukocytes
660   in Lyme carditis. *Infect. Immun.* **75**, 613–20 (2007).

661

662

663

664

665

666

667

668

669 **Acknowledgements**

675

676 **Author Contributions**

677 HHSP performed the all experiments and analyzed the data. JB, a certified MD pathologist

678 helped in histopathology studies, MI performed and analyzed DLS study, AVM performed AFM

679   imaging, KMK helped in fluorescent imaging and *in vivo* studies. HHSP and JR designed the

680   study and wrote the paper. All authors read and approved the final manuscript.

681

682   **Conflict of Interest**

683   Jayakumar Rajadas are listed on the following patent titled "Methods and drug compositions for

684   treating Lyme disease" under international patent application no WO2017124080A1. All other

685   authors report no conflicts of interest in this work.

686

687

688

689

690

691

692   **Legends to Figures**

693   Figure 1: Evaluation of borreliacidal activity of disulfiram (in DMSO and cyclodextrin) with

694   doxycycline as control. A 4 day-old, *B. burgdorferi* log phase culture of *B. burgdorferi* was

695   incubated for four days with disulfiram (Dis-DM), disulfiram (Dis-CD) and doxycycline (Doxy)

696   at the same drug concentrations of 100μM to 0.625μM respectively. After a five-day incubation,

697   bacteria cell viability was assessed by **A**, Bac-titer glow assay. **B**, by direct counting using dark

698   field microscopy and **C**, by SYBR Green-I/PI assay using fluorescent microscopy.

699   Representative images were taken using SYBR green-fluorescent stain (live organisms) and

700   propidium iodide red-fluorescent stain (dead organisms) at 20X magnification. All these

701   experiments were repeated atleast three times. Error bars represent standard errors.

702

703   Figure 2: Evaluation of borreliacidal activity of disulfiram (in DMSO and cyclodextrin) with

704   doxycycline as control. An eight day-old, *B. burgdorferi* log phase culture of *B. burgdorferi* was

705   incubated for four days with disulfiram (Dis-DM) disulfiram, (Dis-CD) and doxycycline (Doxy)

706   at the same drug concentrations of 100μM to 0.625μM respectively. After a five-day incubation,

707   bacteria cell viability was assessed by **A**, Bac-titer glow assay. **B,** by direct counting using dark

708   field microscopy and **C**, by SYBR Green-I/PI assay using fluorescent microscopy.

709   Representative images were taken using SYBR green-fluorescent stain (live organisms) and

710   propidium iodide red-fluorescent stain (dead organisms) at 20X magnification. All these

711   experiments were repeated atleast three times. Error bars represent standard errors.

712

713   Figure 3: Borrelia loads in various tissues after C3H-HeN mice infection followed by disulfiram

714   or doxycycline antibiotics treatment. **A.** Antibiotic treatment/borrelia infection schedule: groups

715   of 5 week old C3H mice (n = 30) were infected subcutaneously above the shoulders with mid log

716   phase 10^5 *B. burgdorferi*. Infected groups were received intraperitoneal antibiotics [doxycycline

717   (n=5), disulfiram (n=5) and PBS (n=5)] in two different time points; day-14 post infection and

718   day-21 post infection. Uninfected groups of mice were kept as controls (n=10). **B.** Necropsy at

719   the end of day-21 and day-28, ears, hearts and urinary bladders were collected for determination

720   of the number of *Borrelia* flab per ul of sample by qPCR. **C.** Photomicrographs (40X) of

721   hematoxylin and eosin stained heart sections; arrows depict the mono nuclear leucocyte

722   infiltrates. Statistics by unpaired t test with Welch's correction between drug treated group

723   versus infected group. *$p < 0.05$, ** $p < 0.01$, *** $p < 0.001$, ****$p < 0.0001$.

724

725   Figure 4: Measurement of immunomodulators in hearts of C3H/HeN mice with or without

726   antibiotics treatment by RT-PCR. RT-PCR of pro-inflammatory transcripts (MIP-2, RANTES,

727   TNF-α, IFN-γ and IL-1β) and important protective immunoregulatory transcripts (IL-10, iNOS

728   and NOS-2) in heart. Statistics by unpaired t test with Welch's correction between control versus

729   infected and also between drug treated group versus infected group. *p < 0.05, ** p < 0.01, *** p

730   < 0.001. NS means not significant.

731

732   Figure 5: Antibody response in the serum with and without antibiotics treatment. A. Total

733   concentration of IgA, IgM, IgG, IgG1, IgG2a, IgG2b and IgG3 antibodies day 21 post-infection

734   and B. Total concentration of IgA, IgM, IgG, IgG1, IgG2a, IgG2b and IgG3 antibodies day 28

735   post-infection which were quantified by ELISA. Statistics: unpaired t test with Welch's

736   correction between controls versus infected and between drug treated group versus infected

737   group. *p < 0.05, ** p < 0.01, *** p < 0.001. NS means not significant.

738

739   Figure 6: Percentage of B cells, T cells, CD8+ cytotoxic T cells, CD4+ helper T cells, naïve,

740   effector and memory CD4+ T cells in lymph nodes. Flow cytometric analysis of immune cells

741   isolated from peripheral lymph nodes from uninfected and infected mice treated with antibiotics.

742   Cells were labelled with anti-CD19, anti-CD3, anti-CD4, anti-CD8, anti-CD44 and anti-CD62L

743   lineage surface markers. Statistics unpaired t test with Welch's correction between control versus

744   infected and between drug treated group versus infected group. *p < 0.05, ** p < 0.01, *** p <

745   0.001. NS means not significant.

746

747

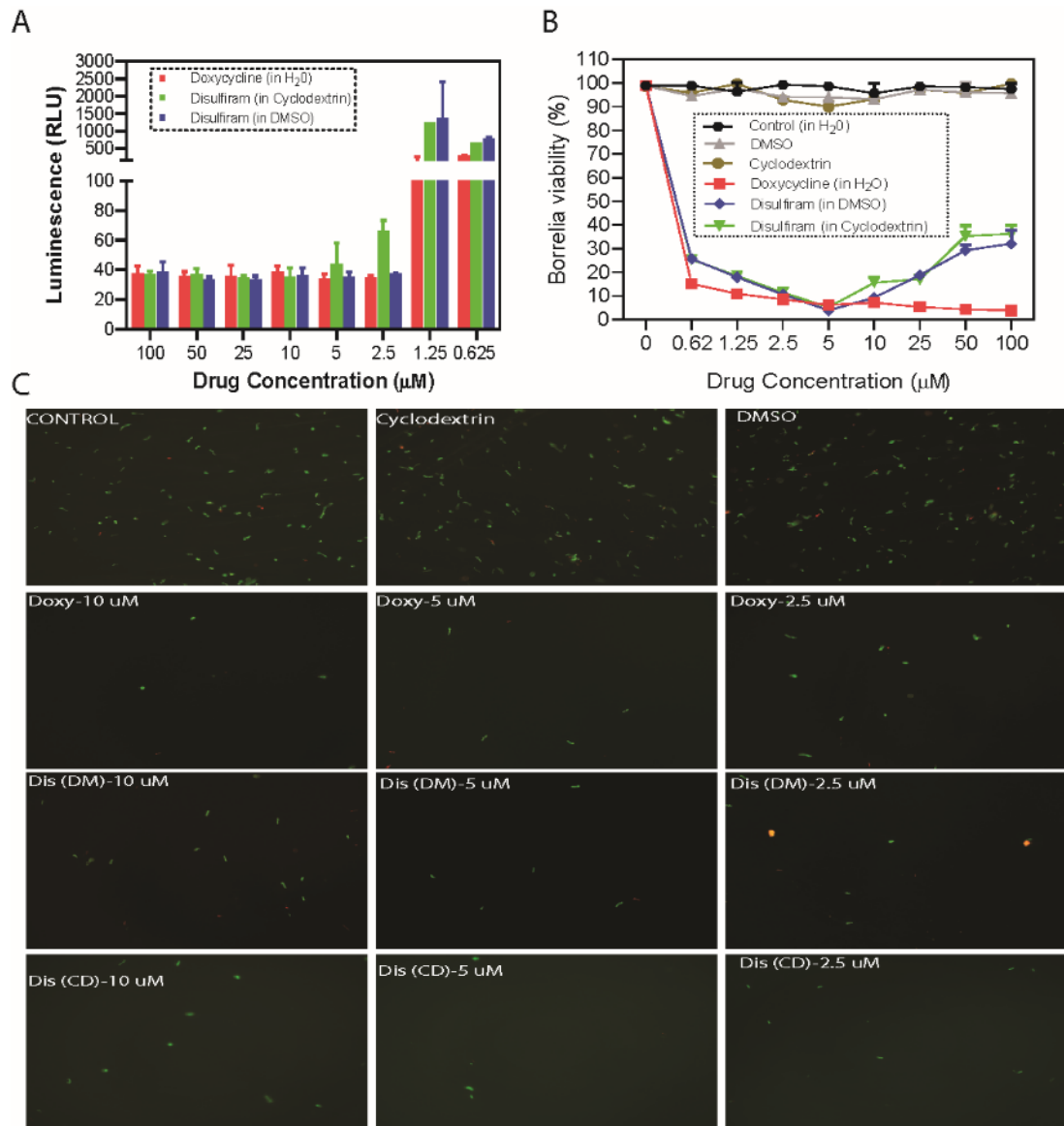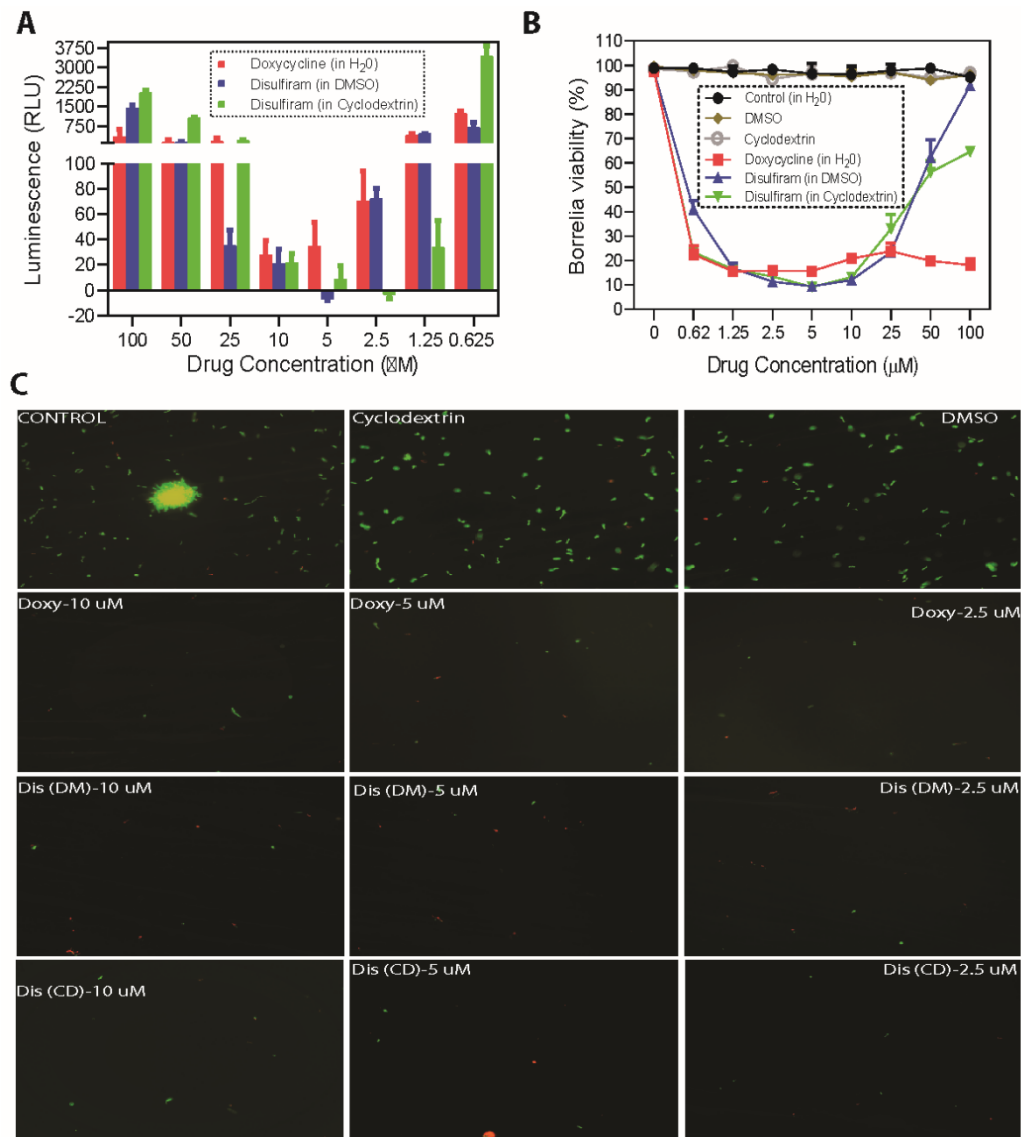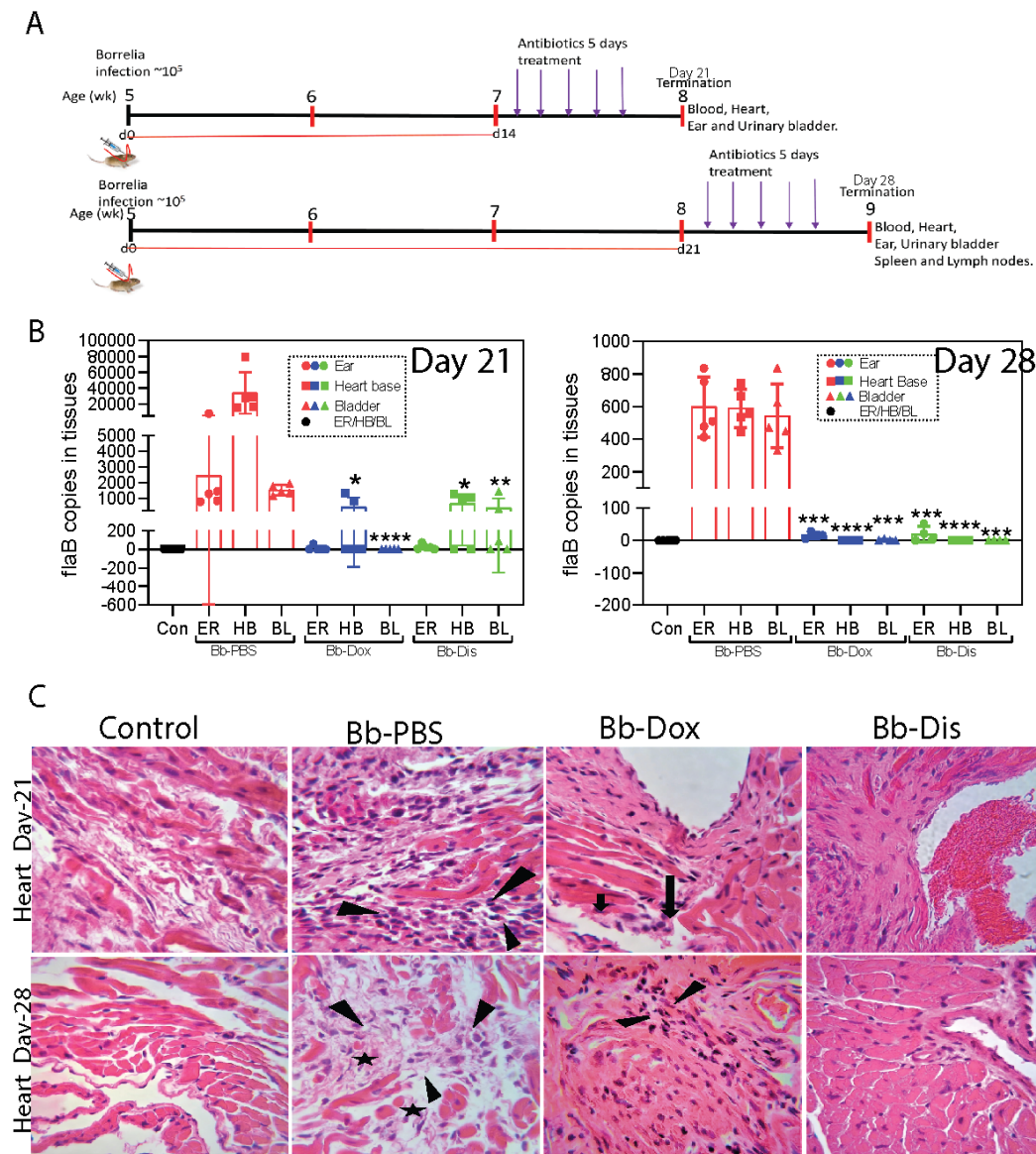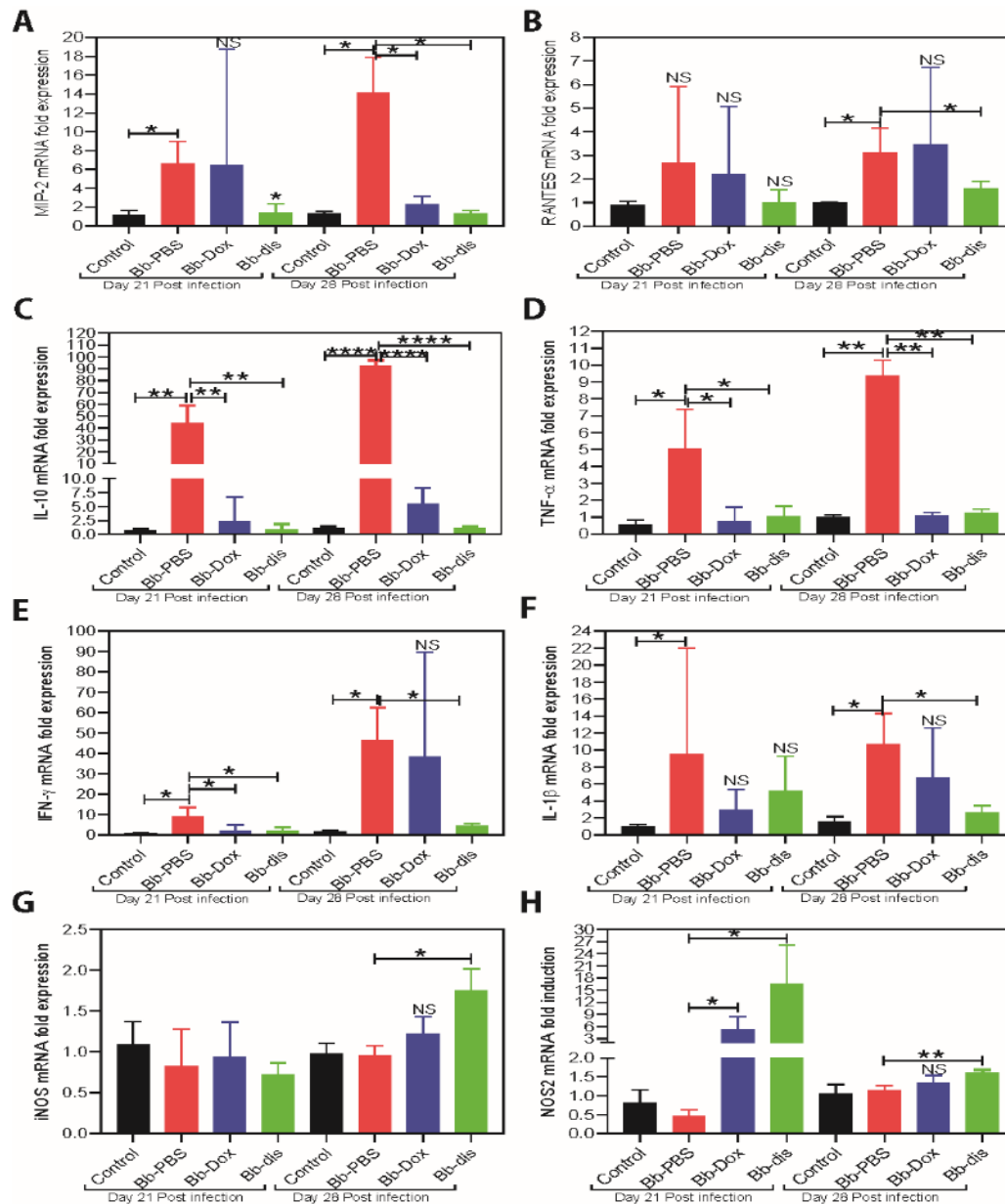748

749

750

751

752

753

754

755

756

757

758

759

760

761

762

763

764

765

766

767

768

769

770

771

772

773

774

775

776

777

778

779
780
781
782
783
784
785
786
787
788
789
790
791
792
793
794
795
796
797
798
799
800
801
802
803
804
805
806
807
808
809
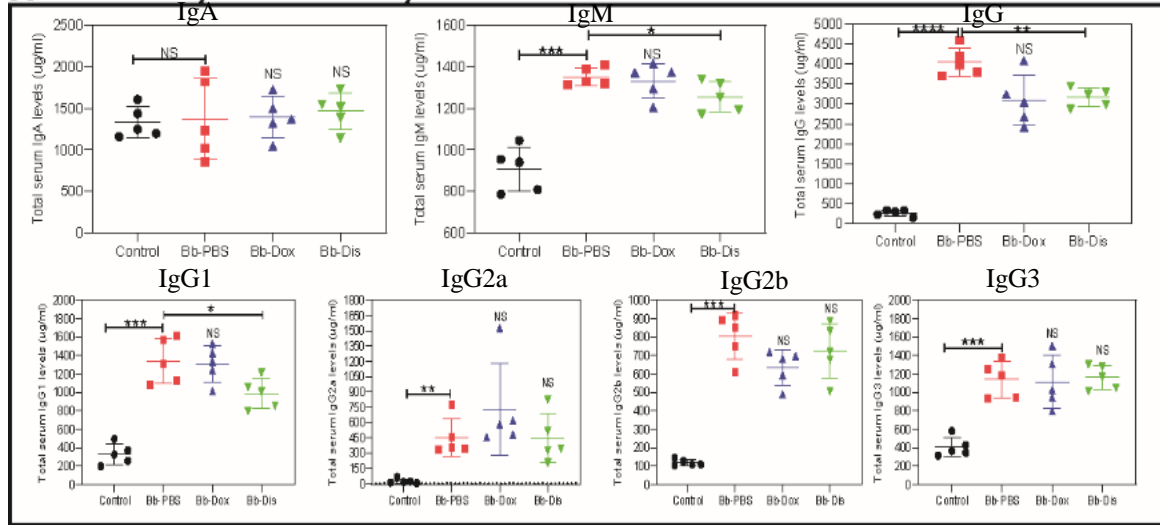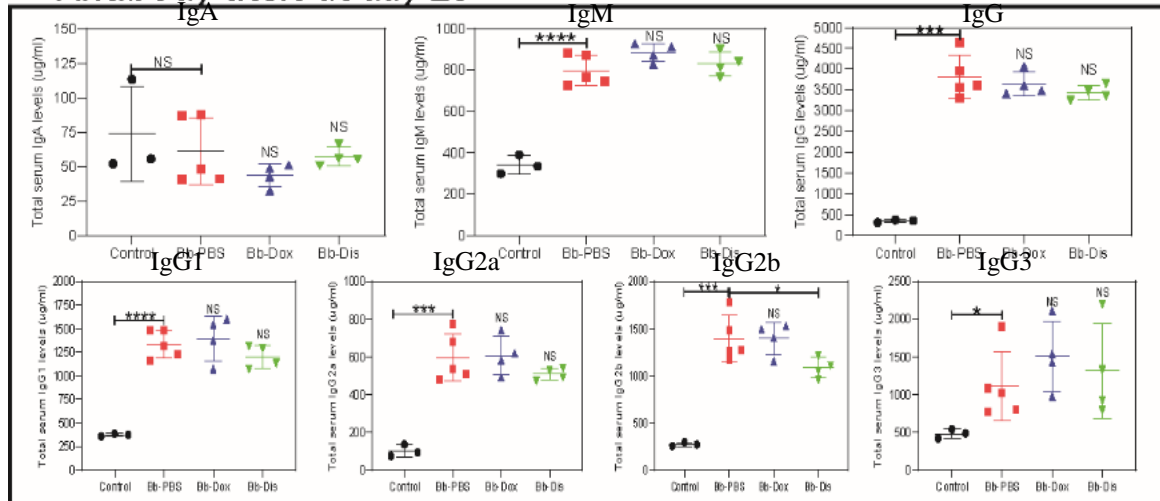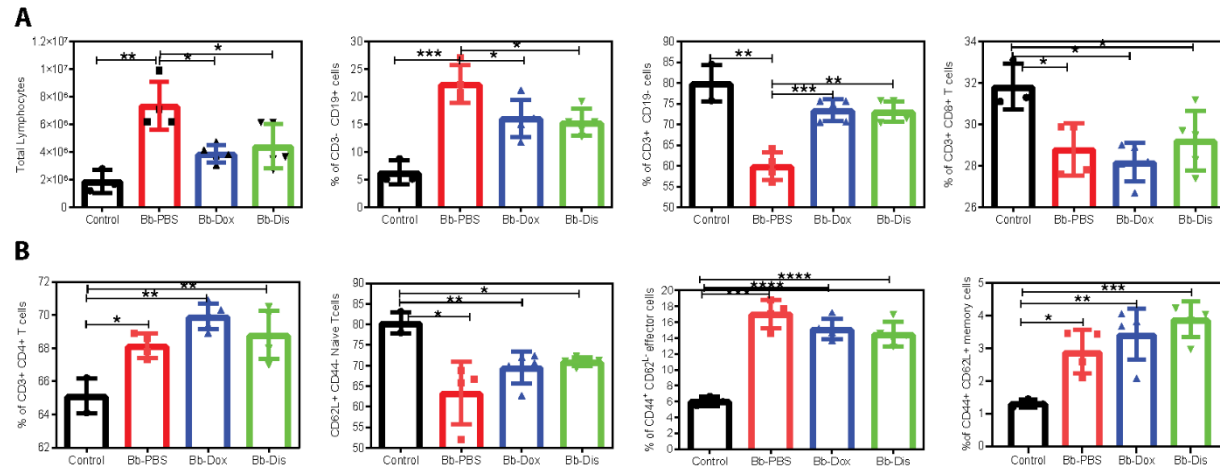
810 **Table 1:** *In vivo* efficacy of drugs against *B. burgdorferi* in C3H/HeN mice. After 14 days of

811 *B.burgdorferi* infection, C3H/HeN mice were treated with following drugs once per day for 5

812 days (Doxycycline – 50 mg/kg and Disulfiram – 75 mg/kg). The whole DNA was extracted from

No. of mice infected	Drug name	No. of *fla-b* DNA copies/Ear	No. of *fla-b* DNA copies/Bladder	No. of *fla-b* DNA copies/Heart
1	Saline (No drug)	847	1761	15893
2		791	1422	28683
3		7851	1335	79512
4		1275	1136	16256
5		1447	1933	28125
1	Doxycycline	0	0	842

813 urinary bladder, ear and heart and further analyzed data by qPCR.

No. of mice infected	Drug name	No. of *fla-b* DNA copies/Ear	No. of *fla-b* DNA copies/Bladder	No. of *fla-b* DNA copies/Heart
2		4	0	12
3		0	0	0
4		56	0	1325
5		10	0	0
1	Disulfiram	73	0	935
2		0	1439	0
3		0	0	1044
4		20	307	1297
1	Saline (No drug)	477	625	447
5		20	89	0

814
815
816
817
818
819
820
821
822
823
824
825
826
827
828 **Table 2:** *In vivo* efficacy of drugs against *B. burgdorferi* in C3H/HeN mice. After 21 days of

829 *B.burgdorferi* infection, C3H/HeN mice were treated with following drugs once per day for 5

830 days (Doxycycline – 50 mg/kg and Disulfiram – 75 mg/kg). The whole DNA was extracted from

831 urinary bladder, ear and heart and further analyzed data by qPCR.

2		509	469	663
3		412	837	534
4		835	448	745
5		753	331	556
1	Doxycycline	28	0	0
2		5	0	0
3		14	6	0
4		15	0	0
1	Disulfiram	0	0	0
2		21	0	0
3		0	0	0
4		51	0	0

832
833
834
835
836
837
838
839
840
841
842
843
844
845
846